International Journal of Science and Research (IJSR)
ISSN: 2319-7064
SJIF (2019): 7.583

Load-Tolerating Capability of the Bearing due to Various Film Shapes of Rough Longitudinal Slider Bearing with Ferro-Lubricant

Girish C. Panchal[1], Himanshu C. Patel[2], Himesh A. Patel[3]

[1]Department of Mathematics, Vishwakarma Government Engineering College, Chandkheda, Gujarat, India
Corresponding Author: *gcpanchal[at]vgecg.ac.in*

[2]Indian Institute of Teacher's education, Gandhinagar, Gujarat, India
dr.prof.hcpatel[at]ldce.ac.in

[3]Department of Mathematics, GPERI, Mehsana, Gujarat, India
himesh.patel4[at]gmail.com

Abstract: ***This paper investigates the effect of various film shapes of rough longitudinal slider bearing with Ferro-lubricant on the bearing system's load-tolerating capability (LTC). The current article describes the efforts to improve bearing's LTC by using a Ferro-lubricant as a non-Newtonian fluid and choosing the bearing's(piston ring's) proper geometrical shape in the I. C. Engine. The mathematical model and the numerical and graphical results reveal the facts about enhancing the bearing system's performance. Moreover, the adverse effect of roughness can be lessened to a certain range by growing the magnetic field's strength.***

Keywords: Averaged Reynolds' type equation (ARTE), Slider bearing, Longitudinal roughness, Ferro-lubricant

Nomenclature

$\overline{b_T}$	Average film thickness (Mean gap) (m)
$f(\delta)$	The frequency density function of combined roughness amplitude δ (m^{-1})
l	Length of slider bearing (m)
w	The load-tolerating capability(LTC) (N)
W^*	The load-tolerating capability(LTC) (Dimensionless)
b_T	Local film thickness (m)
p	Local pressure (N/m^2)
$\bar{p}$	Mean pressure level (N/m^2)
P^*	Mean pressure level (Dimensionless)
b_0	Minimum film-thickness at the trailing edge of slider bearing (m)
b_1	Maximum film-thickness at the winning edge of slider bearing (m)
B_0	Minimum film thickness – Roughness ratio $\frac{h_0}{\sigma}$ (Dimensionless)
b	Nominal (mean) film thickness (m)
B	Nominal film thickness – Roughness ratio $\frac{h}{\sigma}$ (Dimensionless)
$(\bar{p})$	The expected value of the mean pressure level $\bar{p}$ (N/m^2)
V	The velocity of bearing surface in X-Direction (m/s)
ρ	Density of lubricant (Kg/m^3)
α	Mean of random surface roughness (m)
$\alpha*$	Mean of random surface roughness (Dimensionless)
$\varphi_x, \varphi_y, \varphi_X, \varphi_Y$	Pressure flow factors (Dimensionless)
$\delta = \delta_1 + \delta_2$	Random roughness heights of the two surfaces measured from their mean level (m)
φ_s	Shear flow factor (Dimensionless)
ε	The skewness of random surface roughness (m^3)
$\varepsilon*$	The skewness of random surface roughness (Dimensionless)
σ_1, σ_2	Standard deviations of the surfaces (m)
σ	The standard deviation(SD) of random surface roughness (m)
$\sigma*$	The standard deviation of random surface roughness (Dimensionless)
γ	The ratio of X and Y correlation lengths of the surface roughness (Dimensionless)
η	Viscosity of lubricant $(Kg/m.s)$
μ^*	Magnetization parameter (Dimensionless)
μ_0	Magnetic susceptibility
μ_f	Free space permeability $(KgmA^{-2}S^{-2})$

1. Introduction

The Classical lubrication theory establishes the prediction of the bearing's behavior in the sense of friction, wear, roughness pattern parameters (RPP), and load-tolerating capability for the case of Newtonian fluids. In the bearing's system, the roughness and lubricants play a crucial role in getting better performance.

Much research work is done to reduce friction and wear and enrich the performance in an internal combustion engine by design and mechanical point of view. Many investigators [2], [7], [16] analyzed the bearing's life-time and performance to be influenced by friction, wear, lubricants, and surface roughness. The bearing's performance depends on different types of roughness and lubricant [9]-[12]. Many results showing the relationship among the essential parameters like bearing's LTC, mean, SD, skewness, and magnetization parameter are established.

The different types of material combinations can turn out to be a suitable option for the ferrofluid-based journal bearing system and enhance the life-time of the bearing [14]. Some appropriate situations being generated due to the positive effect of ferrofluid help reimburse the low impact of roughness [13].

In these studies, the role of Christensen and Tonder [3]-[6] could not be undervalued who have formed ARTE by smearing the stochastic averaging procedure on "Reynolds' type equation," which provides the mean-pressure more desirable than a local-pressure.

In the present article, the comparison between Plane Shape Slider Bearing (PSB), Hyperbolic Shape Slider Bearing (HSB), Exponential Shape Slider Bearing (ESB), and Secant Shape Slider Bearing (SSB) is analyzed. We used Simpson's 1/3-rule to evaluate the integrals while solving the modified ARTE. It is investigated how the RPP makes variations in the performance of the bearing system in various shapes. It gives the graphical comparison between altered bearing geometries or the geometric shapes (plane, exponential, hyperbolic, and secant) of piston-ring. Moreover, the adverse effect of roughness can be lessened to a specific range by growing the magnetic field's strength.

2. Mathematical Analysis

Patir [15] has presented the ARTE that governs the mean pressure in a rough slider bearing.

$$\frac{\partial}{\partial x}\left[\varphi_x \frac{b^3}{12\eta}\frac{\partial \bar{p}}{\partial x}\right]+\frac{\partial}{\partial y}\left[\varphi_y \frac{b^3}{12\eta}\frac{\partial \bar{p}}{\partial y}\right]=\frac{V}{2}\frac{\partial \bar{b}}{\partial x}+\frac{V\sigma}{2}\frac{\partial \varphi_s}{\partial x} \quad (1)$$

Here the flow is presumed to be steady in the X-direction. Since the surface roughness is longitudinal($\gamma > 1$), the variation in roughness heights in X-direction is minimal (Figure-1), so the effect of φ_s maybe treated as insignificant.

Therefore, Equation (1) is reduced to,

$$\frac{d}{dx}\left[\varphi_x \frac{b^3}{12\eta}\frac{d\bar{p}}{dx}\right]=\frac{V}{2}\frac{d\bar{b}}{dx} \quad (2)$$

The geometry of PSB is shown in Figure-2

$$b(x) = b_0 + (b_1 - b_0)\left(1-\frac{x}{l}\right) \quad (3)$$

The geometry of ESB is shown in Figure-3

$$b(x) = b_1\, Exp\left(-\frac{x}{l}\ln\frac{b_1}{b_0}\right) \quad (4)$$

The geometry of HSB is shown in Figure-3

$$b(x) = b_1\left[1+\frac{x}{l}\left(\frac{b_1}{b_0}-1\right)\right]^{-1} \quad (5)$$

The geometry of SSB is shown in Figure-3

$$b(x) = b_0 \sec\left[\left(1-\frac{x}{l}\right)\sec^{-1}\left(\frac{b_1}{b_0}\right)\right] \quad (6)$$

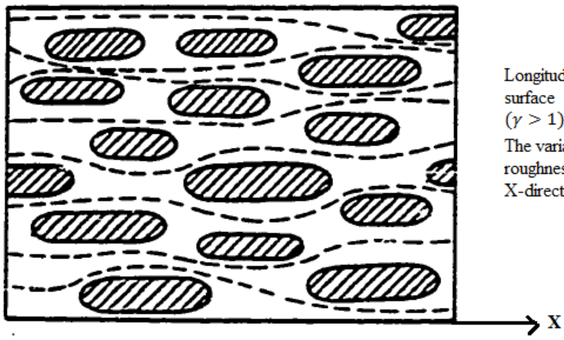

Figure 1: Longitudinal rough surface

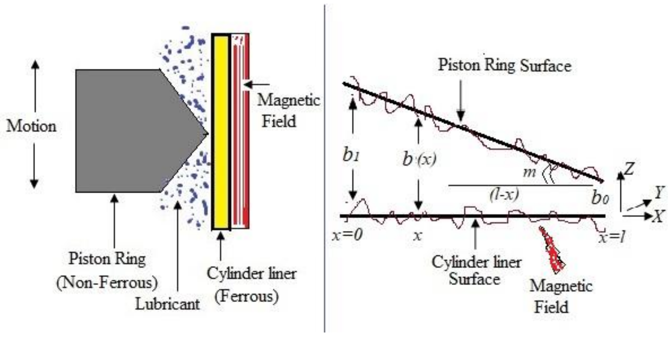

Figure 2: Geometry of PSB

We use the magnetic fluid (Ferro-fluid) instead of any regular lubricant and an external magnetic field produced by an electromagnet or permanent magnet to magnetize the Ferro-fluid. Such magnets can be fixed around the cylinder surface of the piston-ring assembly of an IC engine. Many engineering applications, such as machine tools, gears, sliding contact bearings, clutch plates, etc., use this kind of magnetism.

Applying such magnetic field M having magnitude $M^2=x(l-x)$ slanting to the stable surface of the slider bearing [1] to diminish wear on the sliding material and to get better LTC at the required contact zone. As an outcome of this application, bearing maintenance cost reduces to a substantial extent. The pressure at the contact zone is assumed to be increased concerning the applied magnetism.

Hence the Equation (2) can be modified under the usual assumptions of the hydrodynamic lubrication [1], [8] as:

$$\frac{d}{dx}\left[\varphi_x \frac{b^3}{12\eta}\frac{d}{dx}\left(\bar{p}-0.5\mu_0\mu_f M^2\right)\right]=\frac{V}{2}\frac{d\bar{b}}{dx} \quad (7)$$

International Journal of Science and Research (IJSR)
ISSN: 2319-7064
SJIF (2019): 7.583

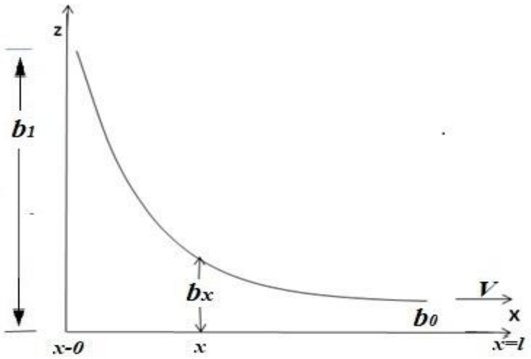

Figure 3: Geometry of HSB, ESB, and SSB

Introducing the mean, variance, and skewness of the surface roughness in the form of expected values [8] as $\alpha=E(\rho)$, $\sigma^2=E[(\rho-\alpha)^2]$, and $\varepsilon=E[(\rho-\alpha)^3]$ respectively. Where, $f(\rho)$, $-c<\rho<c$ is the p.d.f.

Where E(•) represents the expected value of (•) and is defined as

$$E(\bullet)=\int_{-c}^{c}(\bullet)\,f(\delta)d\delta$$

Equation (7) turns into,

$$\frac{d}{dx}\left[\varphi_x\frac{m(b)^{-1}}{12\eta}\frac{d}{dx}\{(\bar{p})-0.5\mu_0\mu_f M^2\}\right]=\frac{V}{2}\frac{d}{dx}[n(b)^{-1}] \tag{8}$$

Where

$$m(b)=b^{-3}[1-3\alpha b^{-1}+6b^{-2}(\sigma^2+\alpha^2)-10b^{-3}(\varepsilon+3\sigma^2\alpha+\alpha^3)]$$

$$n(b)=b^{-1}[1-\alpha b^{-1}+b^{-2}(\sigma^2+\alpha^2)-b^{-3}(\varepsilon+3\sigma^2\alpha+\alpha^3)]$$

Introducing the dimensionless quantities,

$$b^*=\frac{b}{b_0},X=\frac{x}{l},P^*=\frac{b_0^2(\bar{p})}{\eta Vl}$$

$$M(b^*)=b^{*-3}\left[1-3\alpha^*b^{*-1}+6b^{*-2}\left(\sigma^{*2}+\alpha^{*2}\right)-10b^{*-3}(\varepsilon^*+3\sigma^{*2}\alpha^*+\alpha^{*3})\right]$$

$$N(b^*)=b^{*-1}\left[1-\alpha^*b^{*-1}+b^{*-2}\left(\sigma^{*2}+\alpha^{*2}\right)-b^{*-3}(\varepsilon^*+3\sigma^{*2}\alpha^*+\alpha^{*3})\right]$$

We have the non-dimensional form of Equation (8) as,

$$\frac{d}{dX}\left[\varphi_X\,M(b^*)^{-1}\,\frac{d}{dX}\{P^*-\mu^*X(1-X)\}\right]=6\frac{d}{dX}[N(b^*)^{-1}] \tag{9}$$

Where the experimental relation for φ_x is as under [15],

$$\varphi_X=1+C\,B^{-r}=1+C\,(b^*B_0)^{-r}\quad(\text{for }\gamma>1)$$

Where

$$B=\frac{b}{\sigma},\quad B_m=\frac{b_0}{\sigma}$$

And the constants r and C are given [15] as functions of γ in the Table-1.

Table 1: Relation among γ , C, r, and B

γ	C	r	B
3	0.225	1.5	B > 0.5
6	0.520	1.5	B > 0.5
9	0.870	1.5	B > 0.5

Assuming the B.C.: $P^*=0$ at $X=0,\ 1$, and $dP^*/dX=0$, Where the mean gap between two surfaces is maximum, Equation (9) can be turned out to be,

$$P^*(X)=\int_0^X\frac{1}{\varphi_X}\frac{1}{M(b^*)^{-1}}[6\,N(b^*)^{-1}-K^*]dX$$

Where,

$$K^*=\frac{\int_0^1\frac{6\,M(b^*)}{\varphi_X\,N(b^*)}\,dX}{\int_0^1\frac{M(b^*)}{\varphi_X}\,dX}$$

The dimensionless LTC (W^*) per unit width is,

$$W^*=\frac{w.b_0^2}{\mu Vl}=\int_0^1 P^*\,dX \tag{10}$$

$$\therefore W^*=\int_0^1\left[\int_0^X\frac{1}{\varphi_X}\frac{1}{M(b^*)^{-1}}[\,6\,N(b^*)^{-1}-K^*]dX\right]dX$$

3. Results and Discussion

The LTC in dimensionless form is attained by equation (11). Here the integrals throughout the mathematical analysis to get the LTC explicitly are evaluated by Simpson's 1/3-rule, and graphs present the results.

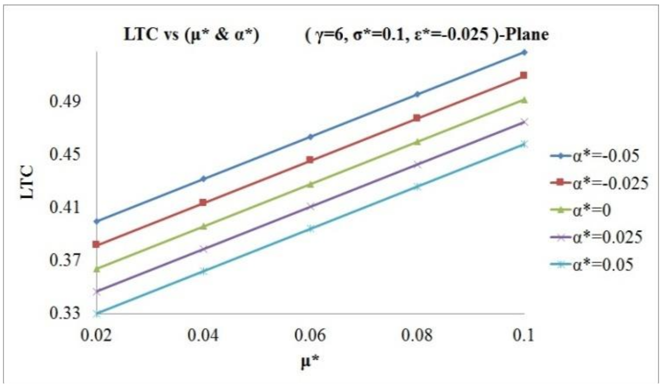

Figure 4: LTC to (μ*and α*): PSB

Figures 4-19 compare the behavior of the dimensionless value LTC of the corresponding bearings concerning different parameters, like mean, SD, skewness, RPP, and magnetism. Observing these results, we can see that the dimensionless LTC's highest value is obtained in the SSB while the PSB produces the least LTC.

In the PSB, the highest value of dimensionless LTC is approximately 0.52 by fixing other parameters as α*=-0.5, σ*=0.1, ε*=-0.025, and γ=6. The LTC increases around from 0.51 to 0.53 while the RPP (γ) moves from 9 to 3. That means that the LTC is higher in the case when the surface is less longitudinal. (Figures 4, 8, 12, 16)

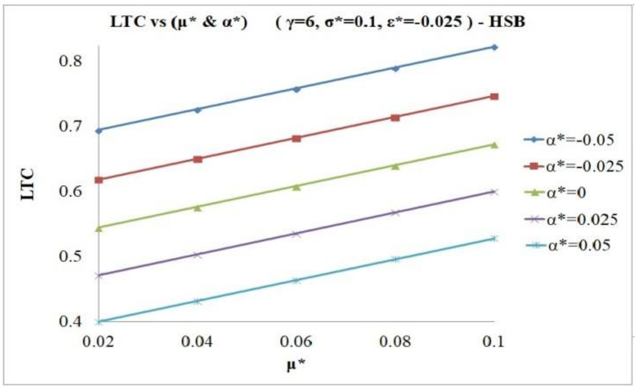

Figure 5: LTC to (μ*and α*): HSB

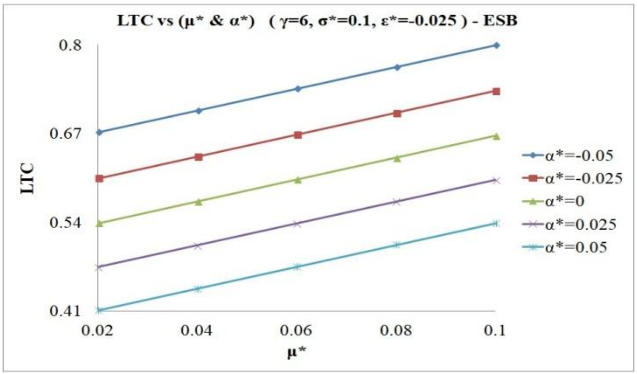

Figure 6: LTC to (μ*and α*): ESB

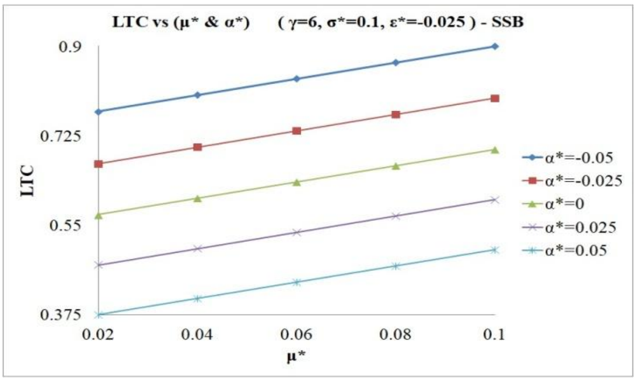

Figure 7: LTC to (μ*and α*): SSB

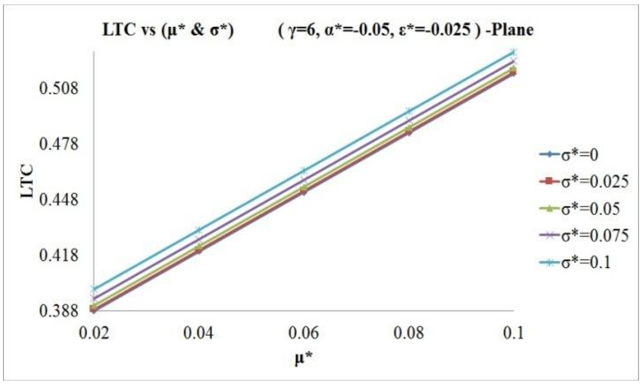

Figure 8: LTC to (μ*and σ*): PSB

In the SSB, the highest value of dimensionless LTC is approximately 0.90 by fixing other parameters as α*=-0.5, σ*=0.1, ε*=-0.025, and γ=6. The LTC increases around from 0.86 to 0.93 while the RPP (γ) moves from 9 to 3. In this case, it also reveals that the LTC is higher in the case when the surface is less longitudinal. (Figures 7, 11, 15, 19)

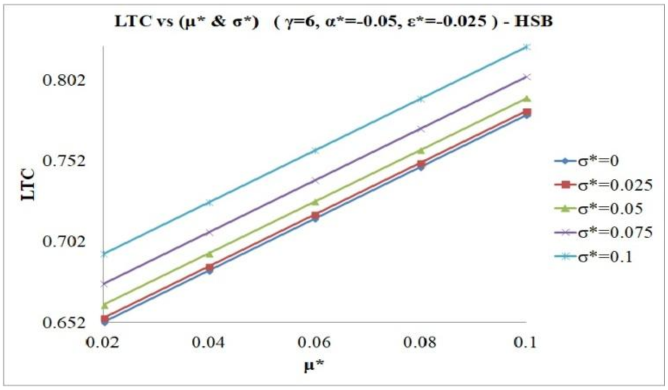

Figure 9: LTC to (μ*and σ*): HSB

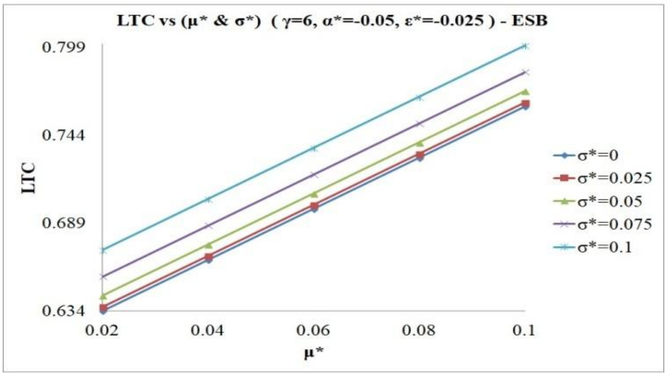

Figure 10: LTC to (μ*and σ*): ESB

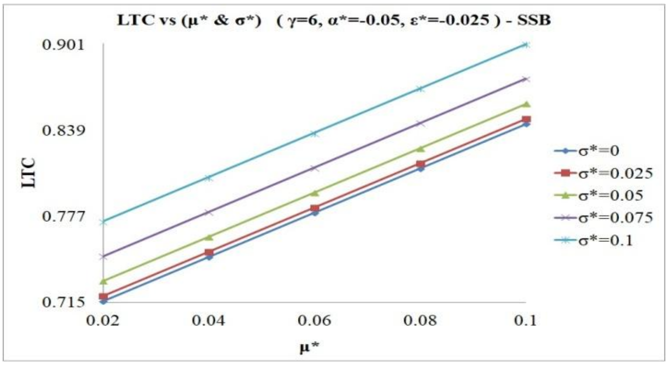

Figure 11: LTC to (μ*and σ*): SSB

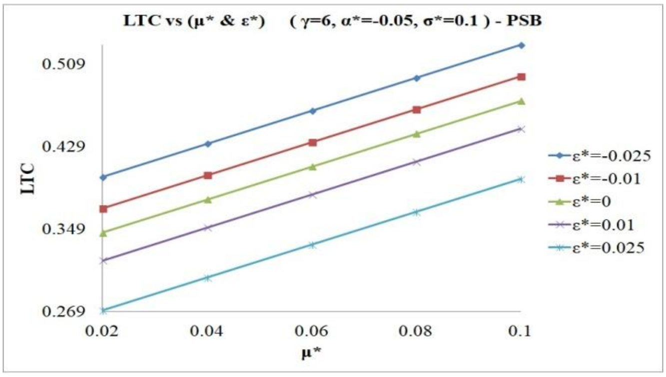

Figure 12: LTC to (μ*and ε*): PSB

In the HSB and ESB, the highest value of dimensionless LTC is approximately 0.82 and 0.80, respectively, by fixing other parameters as α*=-0.5, σ*=0.1, ε*=-0.025, and γ=6. (Figures 5-6,9-10,13-14,17-18)

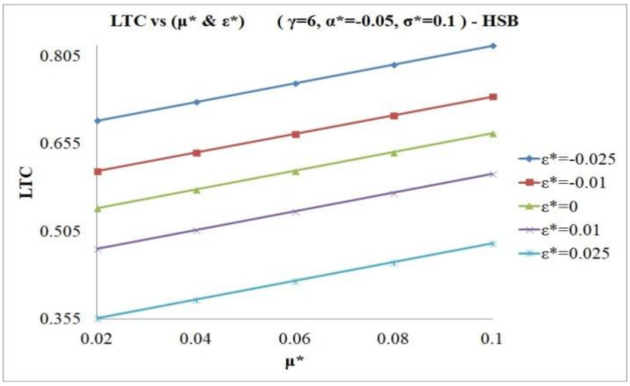

Figure 13: LTC to (μ*and ε*): HSB

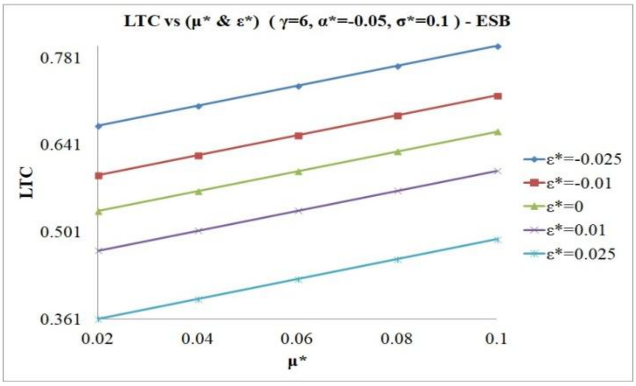

Figure 14: LTC to (μ*and ε*): ESB

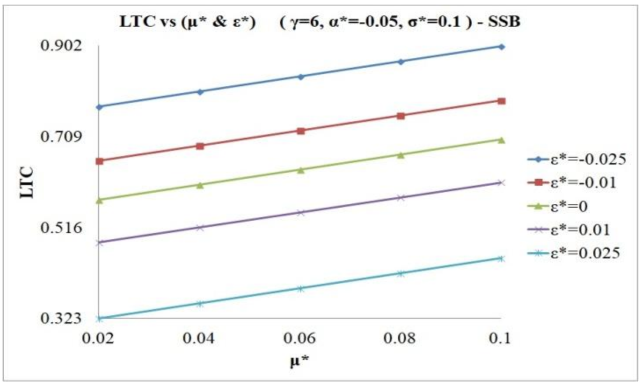

Figure 15: LTC to (μ*and ε*): SSB

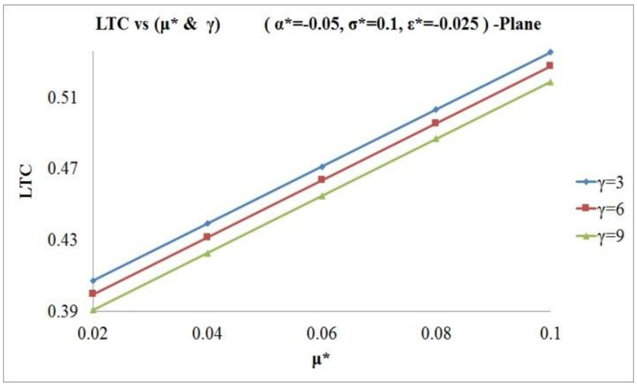

Figure 16: LTC to (μ*and γ): PSB

Figures 4-19 show that the LTC enhances by increasing the values of σ*, α*(-ve), ε*(-ve), and μ*. Hence, the roughness parameters play an important role in improving the bearing's performance irrespective of its shape. The bearing's performance can be more enriched by giving the effect of the magnetic influence, seen in the figures.

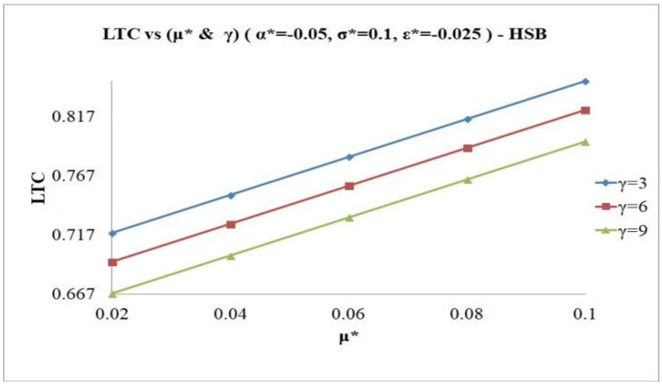

Figure 17: LTC to (μ*and γ): HSB

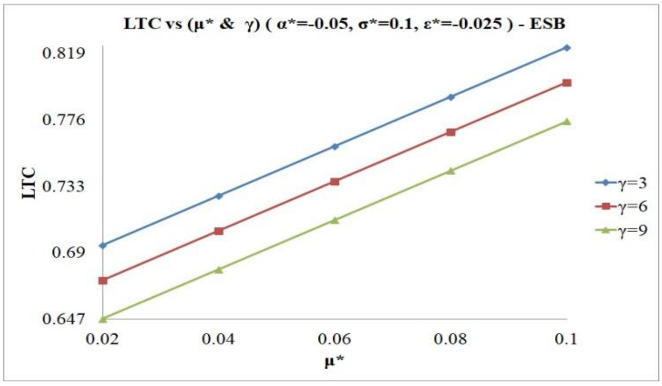

Figure 18: LTC to (μ*and γ): ESB

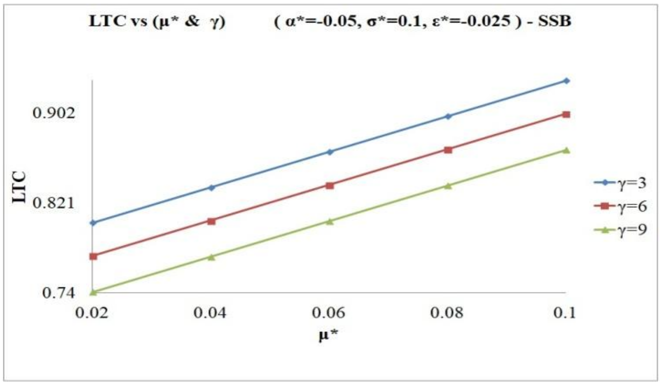

Figure 19: LTC to (μ*and γ): SSB

4. Conclusion

The current analysis asserts that the surface roughness, having negative skewness, negative SD, and large mean produces better LTC regardless of the value of the RPP (γ). The SSB gives better performance than a PSB, HSB, and ESB. It is also to be noted that the LTC can be more boosted by applying the magnetic field at an appropriate area of the bearing system while using the Ferro-lubricant. This study shows that a less longitudinal rough slider bearing with α (-ve) and ε (-ve) can be designed to overcome high friction and wear and achieve superior LTC.

References

[1] Agrawal, V.K., Magnetic-fluid-based porous inclined slider bearing. Wear, 107(2), pp.133–139(1986). DOI:10.1016/0043-1648(86)90023-2.

[2] Burton, R. A., Effects of two-dimensional, sinusoidal roughness on the load support characteristics of a lubricant film. Journal of Fluids Engineering vol.85.2, pp.258-262 (1963).
[3] Christensen H., A Theory of Mixed Lubrication, Proceedings of the Institution of Mechanical Engineers, vol. 186 no. 1 pp.421-430(1972).
[4] Christensen H., Stochastic Models for Hydrodynamic Lubrication of Rough Surfaces, Proceedings of the Institution of Mechanical Engineers, vol. 184 no. 1 pp.1013-1026(1969).
[5] Christensen H., Tonder K., The Hydrodynamic Lubrication of Rough Bearing Surfaces of Finite Width, J. of Lubrication Tech, 93(3), pp.324-329(1971).
[6] Christensen H., Tonder K., Waviness and Roughness in Hydrodynamic Lubrication, Proceedings of the Institution of Mechanical Engineers, vol. 186 no. 1 pp.807-812(1972).
[7] Davies, M. G., The generation of pressure between rough fluid lubricated, moving, deformable surfaces. Lubr. Eng. vol.19, p.246 (1963).
[8] Deheri, G.M., Andharia, P.I., Patel, R.M., Longitudinally rough slider bearings with squeeze film formed by a magnetic fluid, Industrial Lubrication and Tribology, Vol. 56 Issue: 3, pp.177 – 187(2004).
[9] Panchal, G.C., Deheri, G.M., Patel, H.C., Comparative study of various film shapes on the performance of a longitudinal rough finite slider bearing through a series of flow factors. Mathematics Today: An International Journal for Mathematical Sciences, vol. 34(A), pp.40-52 (2018).
[10] Panchal, G.C., Deheri, G.M., Patel, H.C., Influence of magnetic fluid through a series of flow factors on the performance of a longitudinally rough finite slider bearing. Global Journal of Pure and Applied Mathematics, vol. 12(1), pp.783-796 (2016).
[11] Panchal, G.C., Deheri, G.M., Patel, H.C., Influence of surface roughness through a series of flow factors on the performance of a longitudinally rough finite slider bearing. Annals of the Faculty of Engineering Hunedoara-International Journal of Engineering, vol. 14(2), pp.227 (2016).
[12] Panchal, G.C., Deheri, G.M., Patel, H.C., The effect of magnetic fluid together with transverse roughness pattern parameters on the performance of a plane slider bearing. Numerical Modelling in Engineering. Springer, Singapore, pp.151-167 (2018). doi.org/10.1007/978-981-13-2273-0_13.
[13] Patel, H. A., Patel, M. P., Patel, H. C., Deheri, G. M., Squeeze-Film Performance in Parallel Rough Circular Disks Lubricated by Ferro-fluid with Non-newtonian Couple Stress Effect. Proceedings of ICATES, pp.111–115(2013). DOI:10.1007/978-81-322-1656-8_9
[14] Patel, N. S., Vakharia, D. P., Deheri, G. M., Patel, H. C., Experimental performance analysis of Ferro-fluid based hydrodynamic journal bearing with a different combination of materials. Wear, 376-377, pp.1877–1884(2017). DOI:10.1016/j.wear.2017.01.113
[15] Patir N., Ëffects of surface roughness on Partial film lubrication using an average flow model based on numerical simulation, Northwestern University, Ph.D. thesis, Chapter-2 (1978).
[16] Tzeng, S.T., Saibel, E., Surface roughness effect on slider bearing lubrication. ASLE Transactions, vol.10(3), pp.334-348 (1967).

Author Profile

Dr. Girish C. Panchal received the B.Sc. and M.Sc. degrees in Mathematics from Hemchandracharya North Gujarat University, Patan, Gujarat in 2004 and 2006, respectively. He qualified NET (JRF) in Mathematical Sciences. He did Ph.D. in the area of Mathematical modeling in Tribology in 2019 from GTU, Gujarat. Since 2008 to till date, he has been teaching Mathematics in various polytechnics and engineering institutes.